Electronic Supplementary Information

Biological active camellia oleifera protein nanoparticles for improving tumor microenvironment and drug delivery

Xiaoping Qian[a], Tinghui Shen[a], Xiaoke Zhang[a], Chongzhi Wang[a], Weibo Cai[b], Rongshi Cheng[a], Xiqun Jiang*[a]

[a] MOE Key Laboratory of High Performance Polymer Materials and Technology, Department of Polymer Science & Engineering, College of Chemistry & Chemical Engineering, and Jiangsu Key Laboratory for Nanotechnology, Nanjing University, Nanjing, 210023, People's Republic of China

[b] Department of Radiology, University of Wisconsin-Madison, Madison, WI 53705, USA

Table of Contents of Supplementary Information

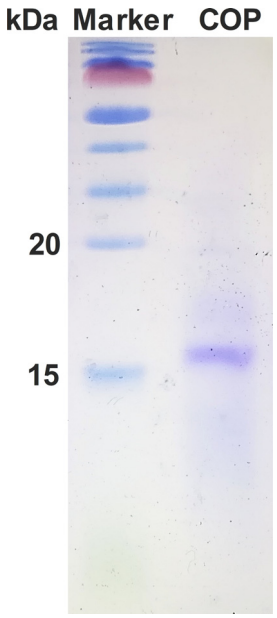

Fig. S1 Sodium dodecyl sulfate polyacrylamide gel electrophoresis (SDS-PAGE) banding patterns of purified COP.

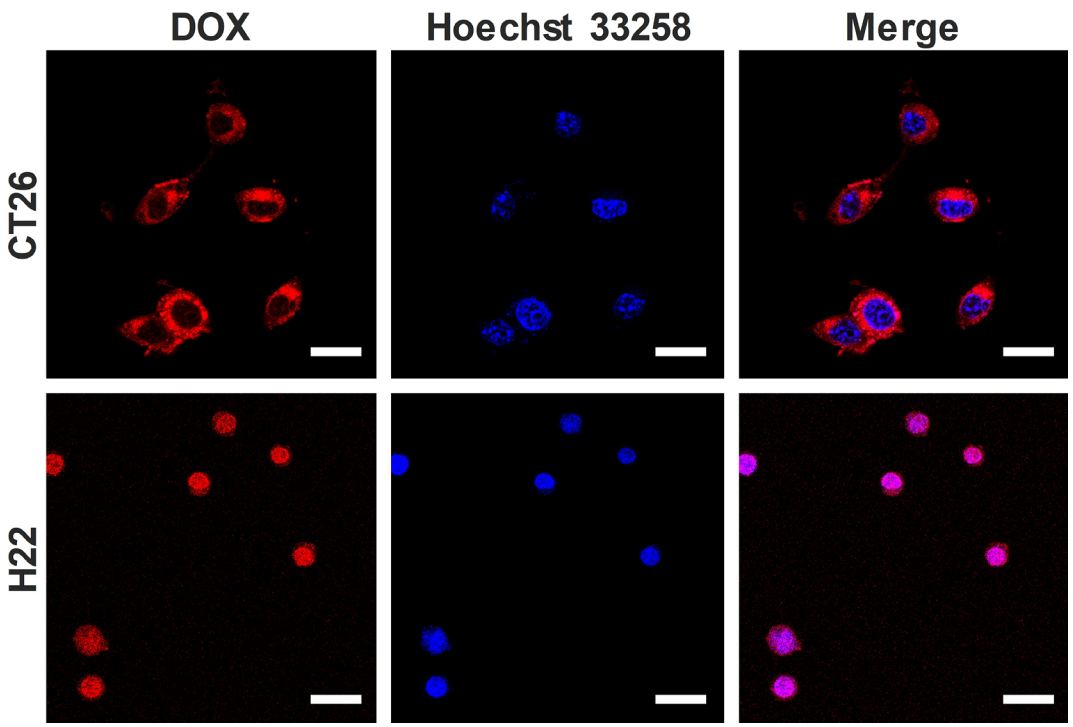

Fig. S2 CLSM images of CT26 and H22 cells incubated with DOX-loaded COP NPs. Red represents DOX and blue represents cell nucleus. Scale bar = 20 μm.

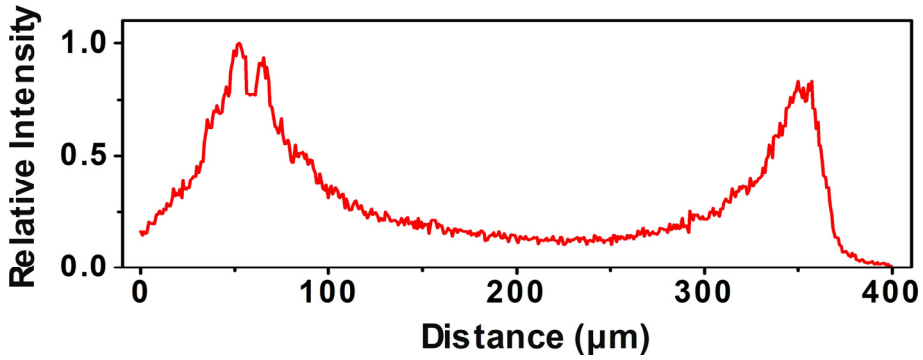

Fig. S3 The penetrate depth of COP NPs in CT26 MCTs measured by ZEN software.

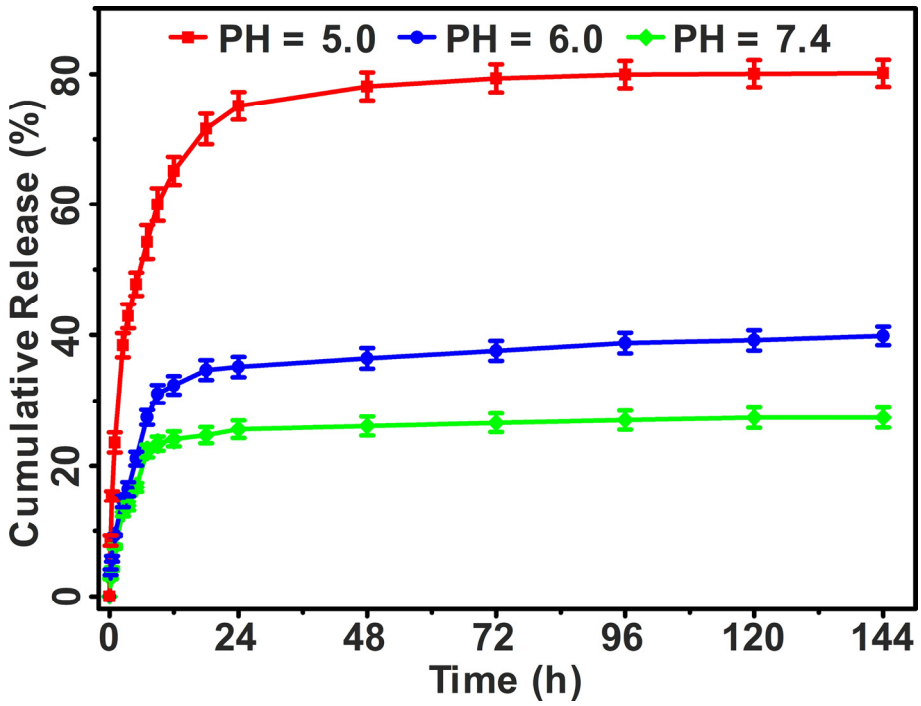

Fig. S4 Drug release profile of DOX from DOX-loaded COP NPs in 0.01 M PBS at PH 5.0, 6.0 and 7.4 at 37 ºC in vitro. Data is represented as mean ± SD (N = 3).

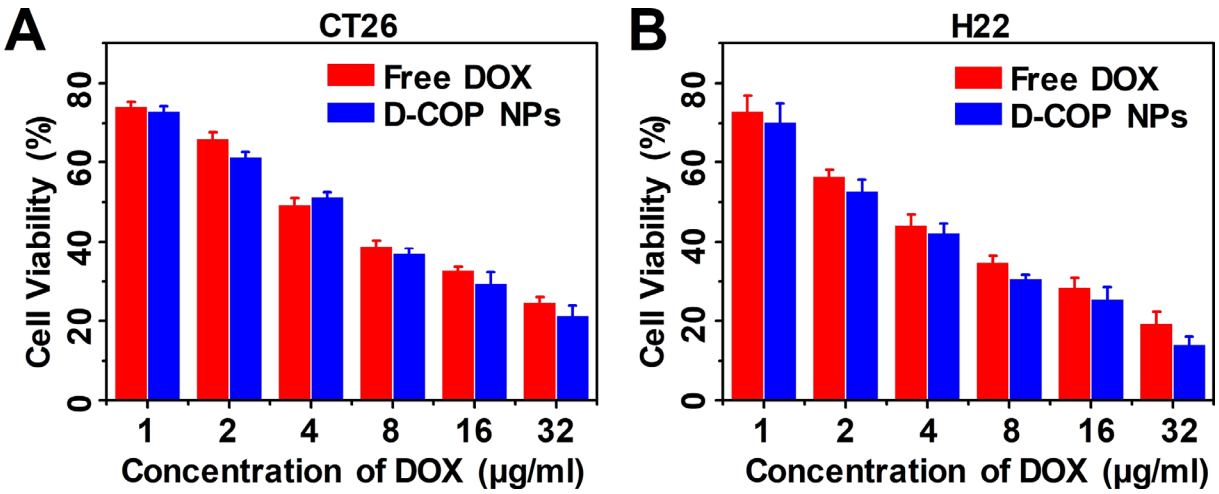

Fig. S5 The cytotoxicity of free DOX and D-COP NPs against (A) CT26 cells and (B) H22 cells after co-cultured for 48 h. Data is represented as mean ± SD (N = 3).

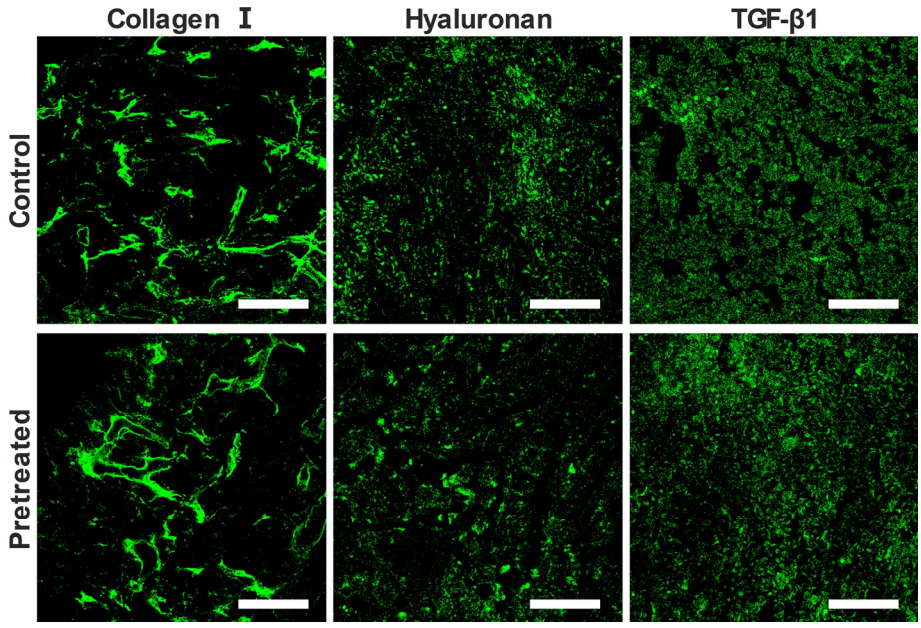

Fig. S6 Confocal laser scanning microscopy (CLSM) images of collagen I, hyaluronan and TGF-β1 of sliced H22 tumor before and after treatment with COP NPs. Scale bar = 100 μm.

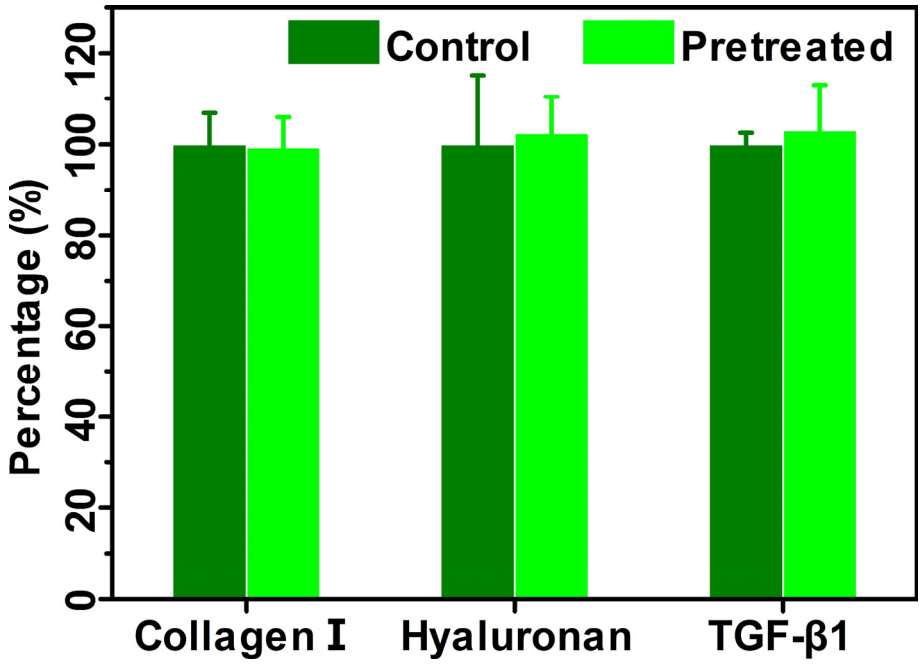

Fig. S7 Semi-quantitative fluorescence intensity calculated from Fig. S3. The control group was normalized as 100% individually.

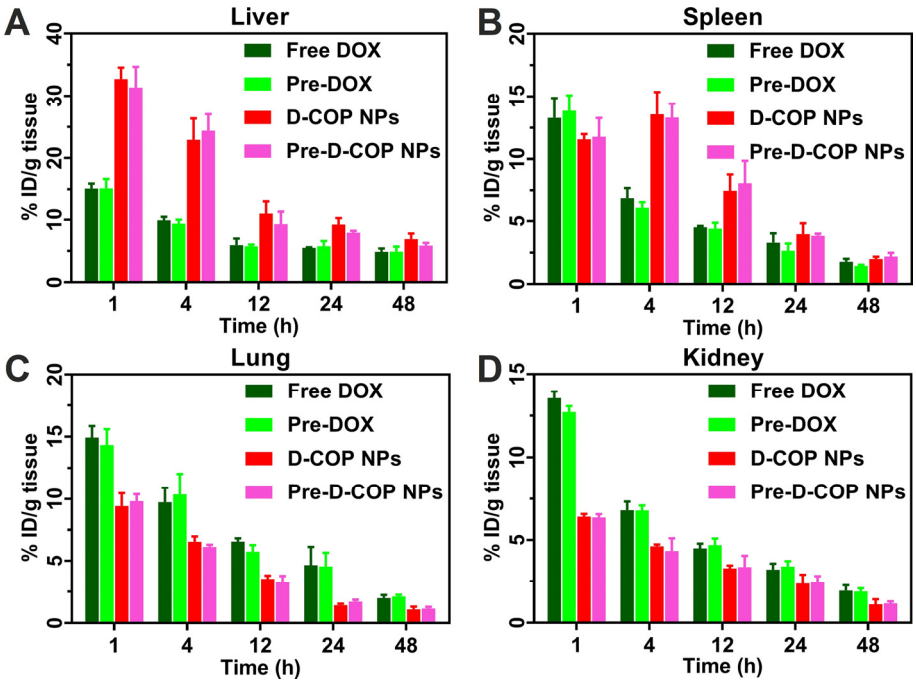

Fig. S8 Biodistribution of DOX in liver (A), spleen (B), lung (C) and kidney (D) of H22 tumor-bearing mice at various time points after i.v. injection of free DOX or D-COP NPs. Data is represented as mean ± SD (N = 3).